Journal of Biomechanics xxx (xxxx) xxx

Contents lists available at ScienceDirect

Journal of Biomechanics

journal homepage: www.elsevier.com/locate/jbiomech
www.JBiomech.com

# Reorienting the tibial baseplate improves the registration accuracy of model-based radiostereometric analysis

Abigail E. Niesen [a], Anna L. Garverick [a], Stephen M. Howell [a], Maury L. Hull [a,b,c,*]

[a] Department of Biomedical Engineering, University of California, One Shields Avenue, Davis, CA 95616, USA
[b] Department of Mechanical Engineering, University of California, One Shields Avenue, Davis, CA 95616, USA
[c] Department of Orthopaedic Surgery, University of California Davis Medical Center, 4860 Y Street, Suite 3800, Sacramento CA, 95817, USA

ARTICLE INFO

*Article history:*
Accepted 16 October 2020
Available online xxxx

*Keywords:*
Total knee replacement
Tibial baseplate migration
Biplanar radiographs
Model registration
Maximum total point motion

ABSTRACT

Accuracy of model-based radiostereometric analysis (MBRSA) in calculating tibial baseplate migration depends on baseplate shape and orientation relative to the imaging planes. The primary objectives were to introduce a new method for determining the optimal baseplate orientation to minimize bias error during MBRSA and to demonstrate the clinical usefulness of the method using a knee positioning guide to repeatably orient the baseplate. A tibia phantom was rotated to achieve 24 different orientations with three pairs of radiographs acquired at each orientation. Radiographs were processed in MBRSA software and the mean maximum total point motion (MTPM), an indicator of bias error during model registration, was plotted as a function of the rotation angles to determine the optimal orientation and a range of acceptable orientations. The bias error decreased 85% between the reference orientation and the optimal orientation. An acceptable range of orientations was defined by a decrease in bias error more than 50%. Future researchers can use this method to determine the optimal orientation and a range of acceptable orientations for their specific baseplate to minimize bias error. Clinical usefulness was demonstrated by repeatedly imaging a knee model placed in a knee positioning guide (simulated clinical positioning) and demonstrating that the mean orientation ± one standard deviation fell within the acceptable range of orientations. Thus, use of a knee positioning guide was an effective tool for repeatable patient positioning and should be considered for future RSA studies to maintain consistent positioning during a longitudinal study.



## 1. Introduction

Radiostereometric analysis (RSA) is a well-known method for measuring the *in vivo* migration of an implant from a host bone through the acquisition of uniplanar or biplanar radiographs (Henricson and Nilsson, 2016; Koppens et al., 2019; Selvik, 1989; van Hamersveld et al., 2019). Focusing on migration of the tibial baseplate after total knee arthroplasty (TKA), radiopaque bone markers are placed in the trabecular bone of the patient's proximal tibia to establish a local bone-based coordinate system. For determining the position and orientation of the tibial baseplate relative to the host bone, two methods exist. In marker-based RSA, the position and orientation are determined from small markers fixed to the baseplate or insert. In contrast, model-based RSA (MBRSA) eliminates the baseplate markers and determines the position and orientation by registering the projection of a 3D model of the baseplate onto each radiograph (Kaptein et al., 2004; Kaptein et al., 2003; Valstar et al., 2001). MBRSA has been preferred over marker-based RSA since it eliminates the need to fix markers to the baseplate or insert and eliminates the risk of occluding baseplate markers during radiograph acquisition (Kaptein et al., 2003; Karrholm et al., 2006; Valstar et al., 2001). Despite these benefits, the accuracy of marker-based RSA is still superior to MBRSA due to the differing methods of registration (Kaptein et al., 2007; Kaptein et al., 2003).

Focusing attention on MBRSA, an important consideration in maximizing accuracy in the registration process concerns the shape of the baseplate and its orientation relative to the imaging planes. Previous researchers have recognized the importance of implant shape on the accuracy of MBRSA by investigating different types of 3D models, 3D model quality, and uniplanar vs. biplanar set-ups (Kaptein et al., 2003; Prins et al., 2008; Seehaus et al., 2013; Trozzi et al., 2008). Additionally, baseplates with different

* Corresponding author at: Department of Orthopaedic Surgery, University of California Davis Medical Center, 4860 Y Street, Suite 3800, Sacramento CA, 95817, USA.
*E-mail address:* mlhull@ucdavis.edu (M.L. Hull).

https://doi.org/10.1016/j.jbiomech.2020.110078
0021-9290/

designs (e.g. pegged vs. stemmed) have unique features such that the baseplate orientation relative to the imaging planes determines what features are visible during registration.

For a biplanar set-up, the imaging planes are aligned with the laboratory coordinate system defined by a calibration cage such that there is an X-Y imaging plane (coronal view) and a Y-Z imaging plane (sagittal view). If the baseplate is oriented such that its coordinate system axes align with those of the laboratory coordinate system, then features unique to a particular baseplate might be hidden, thus making MBRSA registration difficult and increasing the error for calculated migrations (Fig. 1A). In contrast, orienting the baseplate such that its coordinate system is rotated relative to the laboratory coordinate system might allow unique features to become visible and increase the accuracy of calculated migrations (Fig. 1B).

Prior to starting a clinical RSA study, a phantom study is recommended to determine the accuracy of MBRSA registration for the particular baseplate (Kaptein et al., 2007). However, the phantom study protocol does not include a method for determining the optimal orientation, or range of acceptable orientations, of the baseplate which minimizes errors in computed migrations. Accordingly, the primary objective of this study was to present such a method and apply the method using an example baseplate. Additionally, in clinical RSA studies of the knee or hip, it is important to position the patient in a repeatable orientation during all follow-up radiograph acquisitions (Kaptein et al., 2003; Lindgren et al., 2020; Muharemovic et al., 2017). Thus, another objective was to demonstrate the ability of a knee positioning guide to repeatably orient the baseplate in the clinical setting within the acceptable range of orientations. Furthermore, since the proposed method for determining the optimal orientation uses highly controlled mechanisms in the laboratory for positioning the baseplate while the knee positioning guide uses more realistic clinical positioning mechanisms, the final objective was to compare the bias error for laboratory positioning versus clinical positioning.

## 2. Methods

Seven tantalum bone markers (1 mm diameter) were inserted into the proximal end of a right-side tibia sawbone to create a local bone-based coordinate system. An example baseplate (GMK Sphere, Medacta, Lugano, Switzerland) was rigidly fixed with adhesive to the sawbone so that no relative motion could occur between the bone markers and baseplate. The sawbone-baseplate object (i.e. tibia phantom) was rigidly fixed with adhesive to an L-shaped base, machined from Delrin, which defined the reference orientation in which the axes of the baseplate coordinate system align with the axes of the laboratory coordinate system (Fig. 1A).

The baseplate was rotated about two axes in the laboratory coordinate system to achieve different orientations in the two imaging planes (Fig. 1B). These orientations included all combinations of six rotations about the X-axis and four rotations about the Z-axis (i.e. total of 24 orientations). Positive rotation about the X-axis was controlled precisely by machining five wedges from Delrin at inclinations ranging from 5° to 25° in 5° increments (Fig. 2). Each wedge was machined such that it could be attached to the L-shaped base containing the tibia phantom with screws. Delrin, a radiolucent material, was used to avoid marker or baseplate edge occlusion during radiograph acquisition. Negative rotation about the Z-axis was controlled at angles ranging from 0° to 15° in 5° increments using a protractor circle attached to the base of the calibration cage and aligned with the laboratory coordinate system. Rotations of 25° about the X-axis and 15° about the Z-axis were considered the maximum angles that could be achieved for a large patient's knee given the dimensional constraints of the calibration cage (approximately 28 cm long × 23 cm wide × 23 cm tall). Rotations about the Y-axis were not included since rotation about this axis would not result in features unique to the baseplate becoming visible. Each tested orientation was achieved by applying a space-fixed XZY Euler angle sequence to the baseplate in the laboratory coordinate system. This Euler angle sequence matches the body-

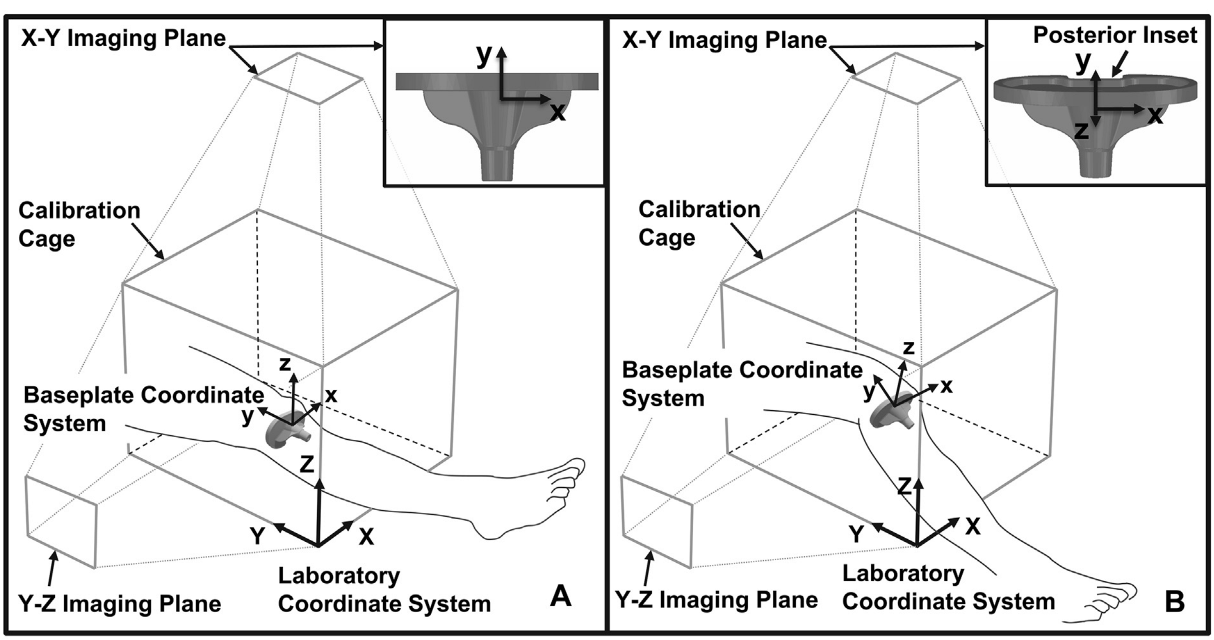


**Fig. 1.** Diagrams of (A) the reference orientation in which the tibial baseplate coordinate system (lowercase) is aligned with the laboratory coordinate system (uppercase) resulting in features unique to the baseplate becoming hidden in the X-Y imaging plane and (B) the tibial baseplate coordinate system rotated positively about the X-axis of the laboratory coordinate system allowing features unique to the baseplate (i.e. posterior inset) to become visible in the X-Y imaging plane. The origin of the baseplate coordinate system is located at the center of mass, the x-axis is oriented in the medial–lateral direction (medial positive for a right baseplate and lateral positive for a left baseplate) such that it is parallel to the posterior inset, the y-axis is oriented perpendicular to the surface of the baseplate (superior direction positive), and the z-axis is oriented in the anterior-posterior direction (anterior positive) such that it is mutually perpendicular to the x and y axes.

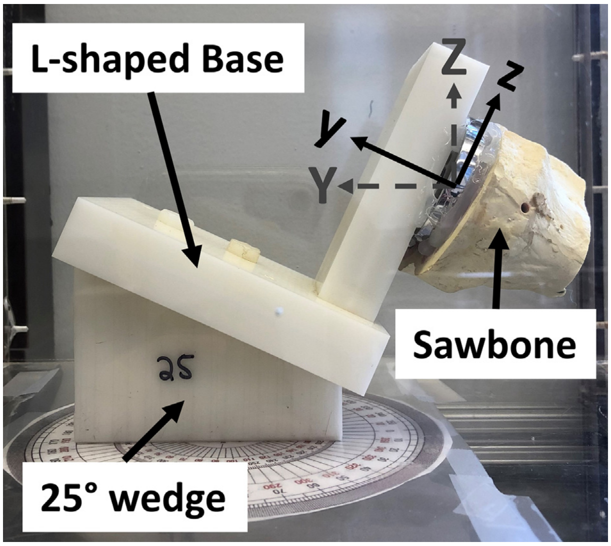


**Fig. 2.** Photograph illustrating how rotations of the tibial baseplate were controlled in laboratory positioning. Positive rotation about the X-axis was controlled by machining five wedges from Delrin at inclinations ranging from 5° to 25° in 5° increments. The 25° wedge is shown in the photograph. Negative rotation about the Z-axis was controlled at angles ranging from 0° to 15° in 5° increments using a protractor circle attached to the base of the calibration cage and aligned with the laboratory coordinate system.

fixed ZXY Euler angles for orienting the CAD model in the MBRSA software (see Appendix). This Euler angle sequence was solely for orienting the baseplate and is independent of the XYZ sequence used to calculate the migration of the baseplate relative to the bone markers (Selvik, 1989). Three independent pairs of radiographs were acquired for each orientation by removing the tibia phantom and attached wedge from the calibration cage and repositioning for Z-axis rotation between exposures.

The imaging equipment consisted of two portable x-ray machines (HF80H+; MinXray, Northbrook, IL) mounted at 90° with respect to one another to view the calibration cage in the X-Y and Y-Z imaging planes. Radiographs were acquired using 80 kVp, 2.7 mAs, and a source-to-image distance of approximately 80 to 100 cm for each x-ray source. A biplanar calibration cage (Model 10; Tilly Medical Products AB, Lund, Sweden) defined the laboratory coordinate system. Radiographs were acquired using two 24 cm by 30 cm cassettes (Fuji IP Cassette type CC) and a computed radiography reader (FCR Carbon XL-2; FUJIFILM Medical Systems U.S.A., Inc., Lexington, MA). The resulting images were 8-bit grayscale with a resolution of 254 dpi.

Images of the tibia phantom were processed using model-based RSA software (version 4.2, RSA*core*, Leiden, The Netherlands). The baseplate CAD model was provided by the manufacturer and reduced to 10,000 facets by the MBRSA software manufacturer. The maximum condition number and mean error of rigid body fitting were 66 and 0.08 mm, respectively, which are well below established guidelines (ISO16087:2013(E), 2013). Three migration values were calculated for each orientation with each pair of radiographs acting as a reference and follow-up time point (i.e. reference-follow-up = 1–2, 2–3, 3–1). Migration was computed as the maximum total point motion (MTPM), which is the greatest movement of any point on the baseplate relative to the bone. Since the baseplate and the sawbone containing the bone markers were rigidly fixed, no relative motion occurred. Thus, the mean MTPM calculated from the three values for each orientation was the bias error (i.e. systematic error) associated with the MBRSA registration for that orientation. The mean MTPM as a function of the rotations about the X-axis and Z-axis was plotted to generate a surface map for identifying the optimal orientation for laboratory positioning (i.e. positioning using the Delrin wedges and protractor), which had the lowest mean MTPM. Additionally, a range of acceptable orientations was identified by determining the orientations which reduced the bias error by more than 50% relative to the reference orientation.

After identifying the optimal orientation and a range of acceptable orientations, a knee positioning guide was manufactured from clear acrylic. An anatomic knee model provided by the baseplate manufacturer and containing all the components of an artificial knee following TKA was used to simulate repeatedly positioning a patient's knee in the clinic using a custom knee positioning guide (Fig. 3). Six tantalum markers (1 mm diameter) were inserted into the acrylic tibia bone at the bottom of drill holes and the baseplate was rigidly fixed with adhesive to the bone. The knee model was placed in the knee positioning guide and biplanar radiographs were acquired. The knee model and positioning guide were removed from the calibration cage and repositioned to acquire ten independent biplanar radiographs. Images of the knee model were processed using MBRSA software and the orientations (i.e. rotations in the laboratory coordinate system about the X, Y, and Z axes) of the CAD model were recorded.

The bias error for simulated clinical positioning of the knee model using the knee positioning guide was determined by calculating the mean MTPM for the ten independent biplanar radiographs with each pair of radiographs acting as a reference and

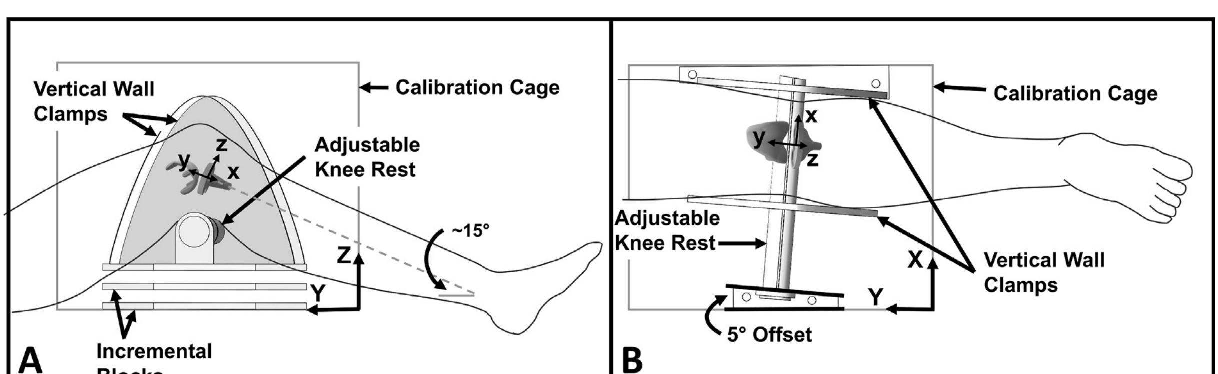


**Fig. 3.** Schematic of knee positioning guide used to simulate clinical positioning by repeatably positioning the knee model within the range of acceptable orientations for (A) Y-Z imaging plane and (B) X-Y imaging plane. Manufactured from acrylic plastic for radiolucency, the knee positioning guide fit snugly into the calibration cage and contained features to control baseplate orientation via knee positioning, including two vertical walls which set the lower limb in 5° valgus (i.e. negative baseplate rotation about the Z-axis) and a knee rest of adjustable height using incremental blocks to control knee flexion (i.e. positive baseplate rotation about the X-axis) using a body-fixed Euler sequence of ZXY.

follow-up time point (i.e. reference-follow-up = 1–2, 2–3, ..., 10–1). The maximum condition number and mean error of rigid body fitting were 33 and 0.07 mm, respectively. To compare the bias error for laboratory positioning versus simulated clinical positioning, the mean MTPMs of the tibia phantom for the four orientations closest to the orientation obtained by the knee positioning guide were pooled (Fig. 4).

### 2.1. Statistical analyses

To determine whether rotations in each imaging plane significantly affected the mean MTPM (1st objective), a two-factor analysis of variance (ANOVA) was performed where the two factors were rotation about the X-axis at six levels and rotation about the Z-axis at four levels (JMP Pro 15, SAS Institute Inc., Cary, NC). The dependent variable was MTPM with three observations for each treatment (i.e. orientation). Additionally, the prediction profiler was used to find the orientation that minimized mean MTPM. Lastly, a post-hoc Tukey pairwise comparison was performed between the reference orientation and the optimal orientation.

To determine whether the knee positioning guide repeatably positioned the knee model within the acceptable range of orientations (2nd objective), the mean rotations ± one standard deviation about the X, Y, and Z axes were determined using the orientation of the CAD model calculated from the MBRSA software.

Lastly, to determine whether the bias error for laboratory positioning versus simulated clinical positioning differed (3rd objective), a Mann-Whitney *U* test was performed between the pooled mean MTPMs from the tibia phantom positioned using highly controlled laboratory means versus the mean MTPM from the knee model positioned using the knee positioning guide.

## 3. Results

For the example baseplate, the mean MTPM was affected by orientation (Table 1). Rotations about the X-axis ($p = 0.001$) and about the Z-axis ($p = 0.02$) were significant. The mean MTPM decreased 85% between the reference orientation and the optimal orientation

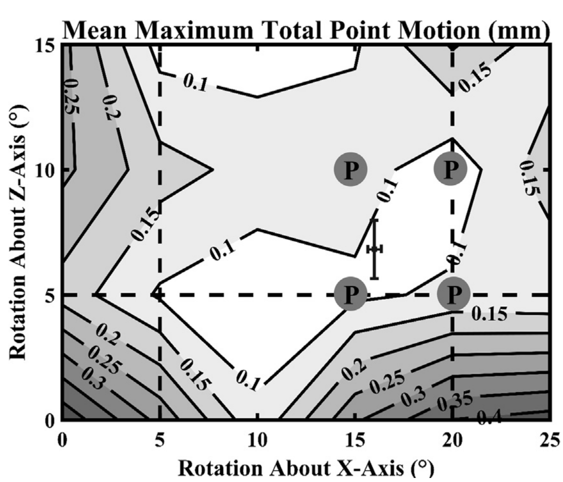


**Fig. 4.** Surface map of the mean maximum total point motion (MTPM) in mm for the three pairs of radiographs acquired at each of 24 orientations for the tibia phantom. The mean MTPM is an indicator of bias error during MBRSA registration since no relative motion occurred between the bone markers and the baseplate. The surface map indicates that the acceptable range of orientations is approximately 5° to 20° rotation about the X-axis and 5° or more rotation about the Z-axis for the example tibial baseplate. The mean orientation ± 1 standard deviation plotted with error bars shows the simulated clinical positioning achieved with the knee positioning guide. The four orientations included in the pooled mean MTPM calculation for the 3rd objective are labeled with P.

(10° rotation about X-axis, 5° rotation about Z-axis) as determined by the prediction profiler. A surface map of the mean MTPM agreed with the result from the prediction profiler (Fig. 4). A post-hoc Tukey pairwise comparison between the reference and optimal orientations showed a significant reduction in mean MTPM (0.437 m m ± 0.17(SD) vs. 0.064 mm ± 0.025, $p = 0.0054$). Since it would be difficult to precisely achieve the optimal orientation in a clinical setting, an acceptable range of orientations was identified (5° – 20° rotation about the X-axis and 5° – 15° rotation about the Z-axis) which reduce the mean MTPM of the MBRSA registration by more than 50% (0.22 mm) (Fig. 4).

The knee positioning guide repeatably positioned the knee model within the acceptable range of orientations (Fig. 4). The Mann-Whitney *U* test showed a significant difference between the pooled mean MTPMs from the tibia phantom using laboratory positioning (i.e. Delrin wedges and protractor) versus the mean MTPM from the knee model using simulated clinical positioning (i.e. knee positioning guide) (0.10 mm ± 0.04 vs. 0.20 mm ± 0.14, $p = 0.03$).

## 4. Discussion

Although the accuracy of MBRSA in calculating baseplate migration depends on the shape of the baseplate and its orientation relative to the imaging planes, this dependency has not been recognized previously and consequently no method has been previously described in the literature for determining the optimal orientation to minimize error during MBRSA registration. Thus, the objectives of this study were to develop a new method for determining the optimal baseplate orientation to minimize bias error during MBRSA registration, demonstrate the clinical usefulness of the method by determining the repeatability of orienting the baseplate within an acceptable range of orientations using a knee positioning guide, and compare the bias error for laboratory positioning (Delrin wedges and protractor) versus simulated clinical positioning (knee positioning guide).

One key result is that the optimal baseplate orientation reduces mean MTPM by up to 85% for an example baseplate. Since it would be difficult to precisely achieve the optimal orientation in a clinical setting, an acceptable range of orientations exist which reduce the mean MTPM of the MBRSA registration by more than 50% (0.22 mm). This reduction in bias is clinically important when comparing mean MTPM to established stability limits, such as the 0.5 mm limit for MTPM at 6 months developed by a recent *meta*-analysis for the phased introduction of new implant designs and/or surgical techniques (Pijls et al., 2018).

A second key result is that the knee positioning guide was effective at repeatably orienting the baseplate with a precision for orientation about the X-axis of 0.1° (i.e. flexion) and rotation about the Z-axis of 1.2° (i.e. valgus). Precision for orientation about the Y-axis (i.e. internal-external rotation) was slightly higher at 2.7° (Table 2), which was expected as there was no feature on the knee positioning guide to control this rotation.

An unexpected result was that the mean MTPM of 0.2 mm for simulated clinical positioning was greater than the pooled mean MTPM of 0.1 mm for laboratory positioning despite similar mean orientations. The mean orientation achieved for simulated clinical positioning was 16° rotation about X and 7° about Z, while the pooled mean orientation achieved with laboratory positioning was 18° rotation about X and 7° about Z (Table 2). An explanation for this result is that the mechanisms for laboratory positioning (Delrin wedges and protractor) more precisely controlled the orientation in contrast to the knee positioning guide, which allowed variability in baseplate orientation more representative of a clinical setting. This explanation was confirmed by noting that the pooled

**Table 1**
Maximum total point motion (MTPM) reported as mean, standard deviation, minimum, and maximum values for the 24 tested tibial baseplate orientations.

| Orientation (°) | | Maximum Total Point Motion (mm) | | | |
|---|---|---|---|---|---|
| X Rotation | Z Rotation | Mean | Standard Deviation | Minimum | Maximum |
| 0 | 0 | 0.44 | 0.17 | 0.30 | 0.63 |
| 0 | 5 | 0.18 | 0.08 | 0.10 | 0.26 |
| 0 | 10 | 0.26 | 0.10 | 0.16 | 0.36 |
| 0 | 15 | 0.26 | 0.21 | 0.07 | 0.48 |
| 5 | 0 | 0.28 | 0.07 | 0.20 | 0.33 |
| 5 | 5 | 0.09 | 0.04 | 0.06 | 0.14 |
| 5 | 10 | 0.17 | 0.06 | 0.10 | 0.21 |
| 5 | 15 | 0.08 | 0.04 | 0.04 | 0.11 |
| 10 | 0 | 0.11 | 0.03 | 0.09 | 0.15 |
| 10 | 5 | 0.06 | 0.02 | 0.04 | 0.09 |
| 10 | 10 | 0.13 | 0.03 | 0.11 | 0.16 |
| 10 | 15 | 0.08 | 0.04 | 0.03 | 0.11 |
| 15 | 0 | 0.29 | 0.20 | 0.07 | 0.42 |
| 15 | 5 | 0.09 | 0.04 | 0.05 | 0.13 |
| 15 | 10 | 0.13 | 0.05 | 0.07 | 0.16 |
| 15 | 15 | 0.09 | 0.03 | 0.06 | 0.12 |
| 20 | 0 | 0.40 | 0.12 | 0.33 | 0.54 |
| 20 | 5 | 0.11 | 0.04 | 0.07 | 0.15 |
| 20 | 10 | 0.06 | 0.03 | 0.04 | 0.09 |
| 20 | 15 | 0.21 | 0.11 | 0.09 | 0.32 |
| 25 | 0 | 0.42 | 0.23 | 0.17 | 0.62 |
| 25 | 5 | 0.10 | 0.04 | 0.06 | 0.14 |
| 25 | 10 | 0.18 | 0.04 | 0.14 | 0.23 |
| 25 | 15 | 0.12 | 0.05 | 0.09 | 0.18 |

**Table 2**
Mean orientation and precision in orientation for simulated clinical positioning (i.e. positioning the knee model using the knee positioning guide) for ten independent biplanar radiographs. For comparison to laboratory positioning (i.e. positioning the tibia phantom using the Delrin wedges and protractor circle), a pooled mean MTPM and pooled precision in orientation were calculated. The pooled orientations included the four orientations closest to the orientation achieved with the knee positioning guide (see Fig. 4).

| | X-axis | Y-axis | Z-axis |
|---|---|---|---|
| Mean Orientation With Simulated Clinical Positioning (°) | 16.2 | 1.1 | 6.8 |
| Precision in Orientation With Simulated Clinical Positioning (°) | 0.1 | 2.7 | 1.2 |
| Pooled Mean Orientation With Laboratory Positioning (°) | 17.8 | −2.3 | 6.7 |
| Pooled Precision in Orientation With Laboratory Positioning (°) | 0.0 | 0.1 | 0.2 |

precision in orientation with laboratory positioning was much better than that obtained with simulated clinical positioning (Table 2). Despite this difference, the knee positioning guide decreased the mean MTPM by more than 50% when compared to the reference orientation.

One reason baseplate orientation may not have been previously investigated to improve MBRSA accuracy is because the ISO standard states that researchers should orient the patient's knee such that the anatomic directions of the knee are aligned as closely as possible with the laboratory coordinate system to obtain clinically relevant migrations (ISO16087:2013(E), 2013). However, this protocol leads to baseplate positioning in the reference orientation, which our results show to have the lowest registration accuracy for the example baseplate studied. Furthermore, anatomic positioning can have substantial variability as demonstrated by a study in which anterior-posterior radiographs of the knee ranged from 8° external to 14° internal rotation relative to the transepicondylar axis despite attempts by the radiologist to position all patients identically (Kawakami et al., 2004). Thus, aligning the patient's knee with the laboratory coordinate system has limitations for both accuracy of model registration and accuracy of anatomic directions.

If the link between anatomic alignment and the laboratory coordinate system is broken to improve registration accuracy, then an alternate coordinate system must be used. For MBRSA, an implant-based coordinate system can be implemented using a feature of the model-based RSA software, RSA*core*. The feature uses the axes attached to the 3D model as the reference coordinate system for the migration calculations and was used in a recent publication in the context of femoral fractures **(**van Embden et al., 2015**).** Implant-based coordinate systems have been proposed in the past in the context of migrating baseplates for marker-based RSA (Laende et al., 2009).

Several advantages accrue to using an implant-based coordinate system for migration calculations instead of anatomic alignment with the laboratory coordinate system. One advantage is that implant-based coordinate systems are defined based on the 3D model and are thus identical for all patients who receive the same implant provided that either the manufacturer's coordinate system is used for CAD models or that a standardized protocol is used to define the directions of the three orthogonal axes for reverse-engineered models. To maintain consistency with the anatomic coordinate system, the directions of the orthogonal axes should adhere to the ISO standard where for a right-sided implant the positive directions are: X = medial, Y = proximal, and Z = anterior which can be obtained for CAD models by applying a transformation to the manufacturer's coordinate system. For reverse engineered models, features of the baseplate should be used to define the axis directions and the methods for defining these directions should be clearly explained to enable other researchers to reproduce the implant-based coordinate system. Furthermore, computed migrations should reference the centroid of the baseplate, rather than the origin of the coordinate system since this is the current standard and has a significant effect on translations (Beardsley et al., 2007; van Hamersveld et al., 2019**).** When adhering to these requirements, use of an implant-based coordinate system will standardize migrations.

One disadvantage in using an implant-based coordinate system surrounds the variability of baseplate rotational alignment which can be substantial during mechanically aligned TKA (Siston et al., 2006). In this case, a postoperative computed tomography scan

can be used to determine a transformation between the implant coordinate system and a joint coordinate system with clinically meaningful motions such as that described by Grood and Suntay (Grood and Suntay, 1983). Baseplate rotational alignment is not a disadvantage for kinematically aligned TKA as studies have demonstrated alignment within ± 11° of the FE plane (Nedopil et al., 2016; Nedopil et al., 2013) which is similar to or less than the variability previously described for patient positioning per the ISO standard.

Another important issue when reorienting the patient's knee is the possibility of marker occlusion. In marker-based RSA studies, use of the reference orientation prevents occlusion of the baseplate markers in the radiographs (Tjornild et al., 2015; Trozzi et al., 2008) whereas in MBRSA studies there are no baseplate markers to occlude. However, at least 3 bone markers in the tibia (for tibial baseplate migration) or in the femur (for femoral component migration) must be visible. Although marker occlusion is a possibility, re-orienting the tibia phantom in this study did not increase tibia marker occlusion. Additionally, since the same positioning will be used during baseline and follow-up imaging, the radiographs will show the same number of markers. The authors did not investigate whether reorienting the knee would affect the occlusion of femoral markers, which is a limitation of the study. If occlusion of femoral markers does occur, then surgeons may need to adopt a different strategy for placing markers in future patients.

Possible orientations included in the method were limited to rotations about the X-and Z-axes since these two axes are perpendicular to the Y-Z and X-Y imaging planes, respectively, in the reference orientation. A positive rotation about the X-axis allowed features unique to the baseplate (mainly an inset on the posterior edge) to become visible (Fig. 5). Clinically, a positive rotation of the baseplate about the X-axis can be achieved by positioning the patient's knee in flexion. A negative rotation of the baseplate about the Z-axis positioned the patient's lower limb in valgus, which allowed the medial and lateral posterior edges of the baseplate to be visualized. Alternatively, a varus rotation could have been used but would not have provided any additional baseplate features. Rotations about the Y-axis were not included in the method since this rotation would not result in features unique to the baseplate becoming visible. Although the method was applied to a right baseplate, the Y-Z imaging plane will always be on the patient's lateral side in which case similar results would be achieved for a left baseplate rotated in flexion and valgus.

Furthermore, the tested orientations were limited to those which could be achieved for patients with large knees given the dimensional constraints of the calibration cage. Based on the authors' experience treating more than 5000 patients with TKA, obtaining knee flexion such that the tibia is angled about 15° from the horizontal (Fig. 3) is achievable postoperatively for almost all patients. If warranted however, then this positioning can be modified for individual patients who are unable to sufficiently flex/extend the knee, and the modified positioning should be retained for that patient at future time points.

When applying this method to other baseplates, the direction of rotation should be chosen such that features unique to the baseplate become visible in the imaging planes. Depending on the set-up of the two x-ray units and type of calibration cage (i.e. biplanar vs. uniplanar), the rotations applied to the baseplate may need to be modified. Additionally, the developed method for determining the optimal baseplate orientation prior to a clinical RSA study may not be necessary for all baseplates. In particular, baseplates containing unique features visible in at least one of the two imaging planes in the reference orientation will not require this method (Fig. 6). However, for baseplates without unique features visible in one of the two imaging planes for the reference orientation, this method is recommended.

Lastly, this study only investigated the registration accuracy of MBRSA for CAD models. If reverse-engineered models had been included, then the accuracy may have been further improved (Kaptein et al., 2003). Accordingly, our results probably represent a worst case for the example baseplate studied.

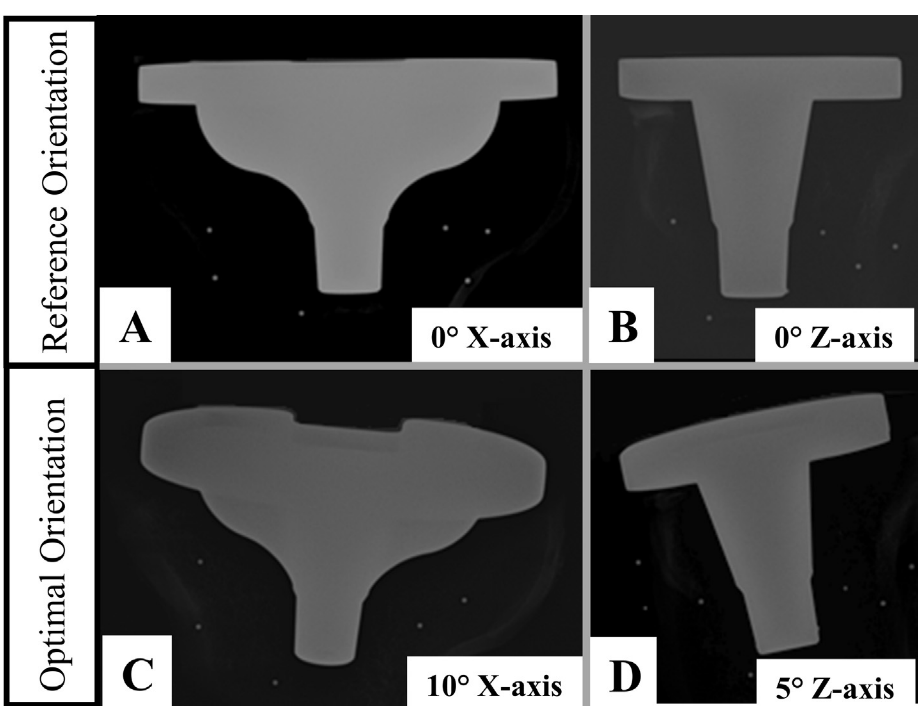


**Fig. 5.** Radiographs showing the reference orientation (i.e. 0° rotation about X-axis and 0° rotation about Z-axis) for (A) X-Y imaging plane and (B) Y-Z imaging plane, and the optimal orientation (i.e. 10° rotation about X-axis and 5° rotation about Z-axis) for (C) X-Y imaging plane and (D) Y-Z imaging plane.

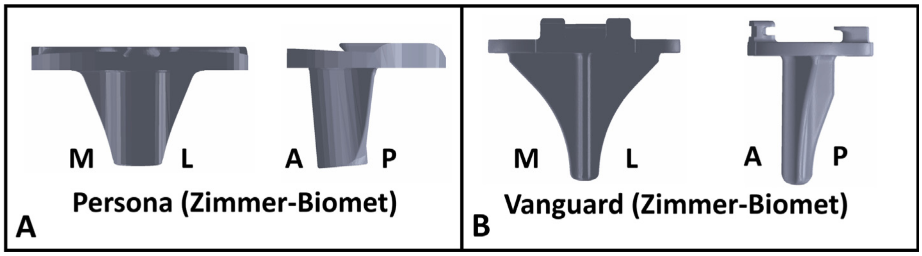


**Fig. 6.** Two additional example tibial baseplates which may or may not require applying the new method for determining the optimal orientation. (A) The Persona tibial baseplate contains minor features unique to the baseplate in the two imaging planes; thus, the new method is recommended. (B) The Vanguard tibial baseplate contains multiple features unique to the baseplate in both imaging planes, thus the new method is not recommended. M = medial, L = lateral, A = anterior, and P = posterior.

## 5. Conclusion

In summary, the results demonstrate that the accuracy of MBRSA depends on the orientation of the baseplate relative to the two imaging planes, and can be significantly improved if the baseplate is rotated relative to the laboratory coordinate system so that features unique to the baseplate are visible. Reorienting the baseplate will require the use of an implant-based coordinate system which is a built-in feature of RSA*core*, thus making it easy to implement. Future researchers can use our method to determine the optimal orientation and a range of acceptable orientations for their specific baseplate to minimize bias error. This reduction in bias error is important when evaluating the performance of new implant designs and/or surgical techniques against established stability limits (Pijls et al., 2018). Furthermore, use of a knee positioning guide was an effective tool for repeatable patient positioning and should be considered for future RSA studies to maintain consistent positioning over the duration of a longitudinal study.

## Acknowledgements

We acknowledge the financial support provided by Medacta. Medacta had no involvement in the study design, collection, analysis, and interpretation of data, or in writing the manuscript.

## Appendix A. Supplementary data

Supplementary data to this article can be found online at https://doi.org/10.1016/j.jbiomech.2020.110078.

## References

Beardsley, C.L., Paller, D.J., Peura, G.D., Brattbakk, B., Beynnon, B.D., 2007. The effect of coordinate system choice and segment reference on RSA-based knee translation measures. J. Biomech. 40, 1417–1422.
Grood, E.S., Suntay, W.J., 1983. A joint coordinate system for the clinical description of three-dimensional motions: application to the Knee. J. Biomech. Eng. 105, 136–144.
Henricson, A., Nilsson, K.G., 2016. Trabecular metal tibial knee component still stable at 10 years. Acta Orthop. 87, 504–510.
ISO16087:2013(E), 2013. Implants for Surgery - Roentgen stereophotogrammetric analysis for the assessment of migration of orthopaedic implants. International Organization for Standardization, Switzerland.
Kaptein, B.L., Valstar, E.R., Stoel, B.C., Reiber, H.C., Nelissen, R.G., 2007. Clinical validation of model-based RSA for a total knee prosthesis. Clin. Orthop. Relat. Res. 464, 205–209.
Kaptein, B.L., Valstar, E.R., Stoel, B.C., Rozing, P.M., Reiber, H.C., 2004. Evaluation of three pose estimation algorithms for model-based Roentgen stereophotogrammetric analysis. J. Eng. Med. 218, 231–238.
Kaptein, B.L., Valstar, E.R., Stoel, B.C., Rozing, P.M., Reiber, J.H.C., 2003. A new model-based RSA method validated using CAD models and models from reversed engineering. J. Biomech. 36, 873–882.
Karrholm, J., Gill, R.H.S., Valstar, E.R., 2006. The history and future of radiostereometric analysis. Clin. Orthop. Relat. Res. 448, 10–21.
Kawakami, H., Sugano, N., Yonenobu, K., Yoshikawa, H., Ochi, T., Hattori, A., Suzuki, N., 2004. Effects of rotation on measurement of lower limb alignment for knee osteotomy. J. Orthop. Res. 22, 1248–1253.
Koppens, D., Rytter, S., Munk, S., Dalsgaard, J., Sorensen, O.G., Hansen, T.B., Stilling, M., 2019. Equal tibial component fixation of a mobile-bearing and fixed-bearing medial unicompartmental knee arthroplasty: a randomized controlled RSA study with 2-year follow-up. Acta Orthop. 90, 575–581.
Laende, E.K., Deluzio, K.J., Hennigar, A.W., Dunbar, M.J., 2009. Implementation and validation of an implant-based coordinate system for RSA migration calculation. J. Biomech. 42, 2387–2393.
Lindgren, L., Jorgensen, P.B., Morup, R.M.S., Jensen, M., Romer, L., Kaptein, B., Stilling, M., 2020. Similar patient positioning: A key factor in follow-up studies when using model-based radiostereometric analysis of the hip. Radiography 26, e45–e51.
Muharemovic, O., Troelsen, A., Thomsen, M.G., Kallemose, T., Gosvig, K.K., 2017. Design and evaluation of learning strategies for a group of radiographers in radiostereometric analysis (RSA). Radiography 23, e80–e86.
Nedopil, A.J., Howell, S.M., Hull, M.L., 2016. Does malrotation of the tibial and femoral components compromise function in kinematically aligned total knee arthroplasty?. Orthop. Clin. North Am. 47, 41–50.
Nedopil, A.J., Howell, S.M., Rudert, M., Roth, J., Hull, M.L., 2013. How frequent is rotational mismatch within 0 degrees +/-10 degrees in kinematically aligned total knee arthroplasty?. Orthopedics 36, e1515–e1520.
Pijls, B.G., Plevier, J.W.M., Nelissen, R., 2018. RSA migration of total knee replacements. Acta Orthop. 89, 320–328.
Prins, A.H., Kaptein, B.L., Stoel, B.C., Nelissen, R.G., Reiber, J.H., Valstar, E.R., 2008. Handling modular hip implants in model-based RSA: combined stem-head models. J. Biomech. 41, 2912–2917.
Seehaus, F., Emmerich, J., Kaptein, B.L., Windhagen, H., Hurschler, C., 2013. Dependence of model-based RSA accuracy on higher and lower implant surface model quality. Biomed. Eng. Online 12.
Selvik, G., 1989. Roentgen stereophotogrammetry. Acta Orthop. Scand. 60 (Suppl), 232.
Siston, R.A., Goodman, S.B., Patel, J.J., Delp, S.L., Giori, N.J., 2006. The high variability of tibial rotational alignment in total knee arthroplasty. Clin. Orthop. Relat. Res. 452, 65–69.
Tjornild, M., Soballe, K., Hansen, P.M., Holm, C., Stilling, M., 2015. Mobile- vs. fixed-bearing total knee replacement. Acta Orthop. 86, 208–214.
Trozzi, C., Kaptein, B.L., Garling, E.H., Shelyakova, T., Russo, A., Bragonzoni, L., Martelli, S., 2008. Precision assessment of model-based RSA for a total knee prosthesis in a biplanar set-up. Knee 15, 396–402.
Valstar, E.R., de Jong, F.W., Vrooman, H.A., Rozing, P.M., Reiber, J.H.C., 2001. Model-based roentgen stereophotogrammetry of orthopaedic implants. J. Biomech. 34, 715–722.
van Embden, D., Stollenwerck, G.A.N.L., Koster, L.A., Kaptein, B., Nelissen, R.G., Schipper, I.B., 2015. The stability of fixation of proximal femoral fractures. Bone Joint J. 97-B, 391–397.
van Hamersveld, K.T., Marang-van de Mheen, P.J., Koster, L.A., Nelissen, R., Toksvig-Larsen, S., Kaptein, B.L., 2019. Marker-based versus model-based radiostereometric analysis of total knee arthroplasty migration: a reanalysis with comparable mean outcomes despite distinct types of measurement error. Acta Orthop. 90, 366–372.